TELKOMNIKA, Vol.10, No.1, March 2012, pp. 55~60
ISSN: 1693-6930
accredited by DGHE (DIKTI), Decree No: 51/Dikti/Kep/2010

Static Characterization of InAs/AlGaAs Broadband Self-Assembled Quantum Dot Lasers

D. Ghodsi Nahri[1], H. Arabshahi*[2]
[1]Department of Physics, Mashhad Branch, Islamic Azad University, Mashhad, Iran
[2]Department of Physics, Payame Noor University, P. O. Box, 19395-3697, Tehran, Iran
e-mail: hadi_arabshahi@yahoo.com

Abstrak

Karakteristik statis dari dioda laser quantum-dot rakitan-sendiri InAs/AlGaAs pita-lebar (SAQD-LDS) telah diteliti dalam makalah ini untuk memecahkan persamaan laju secara numerik menggunakan metode Runge-Kutta orde-empat. Tingkat energi, ukuran, dan komposisi distribusi dari quantum-dots pita-lebar InAs/AlGaAs (QD) dipertimbangkan, pengaruhnya terhadap karakteristik statik diinvestigasi. Hasil simulasi karakteristik statik menunjukkan bahwa nonlinieritas yang muncul dalam karakteristik cahaya-arus dimana ketersebarannya homogen (HB) menjadi sama dengan ketersebaran tak homogen (IHB). Slop-efisiensi meningkat dari HB ke IHB pada degradasi karakteristik cahaya-arus. Faktanya, pita-lebar SAQD-LD InAs/AlGaAs memiliki kinerja terbaik ketika HB sama dengan IHB. Karakteristik cahaya-arus menurun dan arus ambang meningkat seiring peningkatan IHB. Efek cakupan QD pada kinerja laser diinvestigasi, dan menunjukkan bahwa ada cakupan QD optimal di mana SAQD-LD beroperasi dengan arus ambang terendah yang mungkin dan daya keluaran maksimum pada kondisi cakupan QD apapun yang nilainya optimal, arus ambang meningkat dan efisiensi slop menurun.

Kata kunci: *InAs/AlGaAs, homogeneous, inhomogeneous, karakteristik statik, laser quantum-dot*

Abstract

The static-characteristics of InAs/AlGaAs broadband self-assembled quantum-dot laser diodes (SAQD-LDs) have been studied to solve the rate equations numerically using fourth-order Runge-Kutta method. Energy level, size, and composition distributions of the InAs/AlGaAs broadband quantum-dots (QDs) are considered and their effects on Static-characteristics are investigated. Simulated results of static-characteristics show that nonlinearity appears in light-current characteristics whereas homogeneous broadening (HB) becomes equal to inhomogeneous broadening (IHB). Slope-efficiency increases as the HB heightens up to the IHB. Exceeding the HB from IHB results in degradation of light-current characteristics. In fact, InAs/AlGaAs broadband SAQD-LD has the best performance when HB is equal to IHB. Light-current characteristics degrade and threshold current increases as the IHB enhances. We also investigate the effects of QD coverage on the laser performance and show that there is an optimum QD coverage in which the SAQD-LD operates with lowest possible threshold current and maximum output power as whatever the QD coverage enhances from that optimum amount, the threshold current increases and slope efficiency decreases.

Keywords: *InAs/AlGaAs, inhomogeneous, homogeneous, quantum-dot laser, static characterization*

1. Introduction

Three-dimensionally quantum confining medium of electrons,, holes, and excitons in semiconductor microstructures known as quantum dots (QDs) is predicted to produce new physical phenomena and improve optoelectronic devices significantly [1],[2],[[3],[4]. The atom-like state density in QDs associated with three-dimensional confinement of electrons and holes would cause an increase of optical gain and limit thermal carrier distribution. Therefore, the use of QDs for semiconductor lasers as an active region is expected to provide a remarkable reduction of threshold current and temperature sensitivity. During primary research based on predictions in the early 1980s, QDs have been created by combining lithography and re-growth on a processed substrate. The artificial techniques, however, suffer from non-uniform dot size and composition, poor interface quality that cause IHB of optical gain and low numerical density. High uniformity is required to achieve the atom-like state density of a dot ensemble. A high optical quality and high numerical density are required to obtain a large gain [5],[6],[7]. Here, we

Received November 26th, 2011; Revised January 3rd, 2012; Accepted January 9th, 2012

characterize the static features of broadband emitting InAs/AlGaAs self-assembled QD lasers examining the effects of energy level distributions that cause homogeneous broadening (HB) of optical gain and the effects of IHB on the static performance of the mentioned QD lasers. These InAs/AlGaAs QDs exhibit a broad photoluminescence (PL) full width at half maximum (FWHM) of 80 meV, which is much wider than that grown on GaAs substrate and it was proposed that this broadband emission is beneficial for broadening the lasing spectrum [2],[7]. Broadband QD lasers have been observed experimentally [8]. This observation is fundamentally different from conventional quantum-well or bulk lasers characteristics and thus the study of broadband characteristics of QD lasers are necessary to obtain a further insight of the carrier processes in the QD semiconductor materials [9],[10].

2. Simulation Model

Based on the density-matrix theory, the linear optical gain of QD active region is given as

$$g^{(1)}(E) = \frac{2\pi e^2 \hbar N_D}{c n_r e_0 m_0^2} \cdot \frac{\left|p_{cv}^{\sigma}\right|^2 (f_c - f_v)}{E_{cv}} \times B_{cv}(E - E_{cv}) \quad (1)$$

where n_r is the refractive index, N_D is the volume density of QDs, $\left|P_{cv}^{s}\right|^2$ is the transition matrix element, f_c is the electron occupation function of the conduction-band discrete state, f_v is that of the valence-band discrete state, and E_{cv} is the interband transition energy. The linear optical gain shows the homogeneous broadening of a Lorentz shape as

$$B_{cv}(E - E_{cv}) = \frac{\hbar\gamma_{cv} / \pi}{(E - E_{cv})^2 + (\hbar\gamma_{cv})^2} \quad (2)$$

where FWHM is given as $2\hbar\gamma_{cv}$ with polarization dephasing or scattering rate γ_{cv}. Neglecting the optical-field polarization dependence, the transition matrix element is given as

$$\left|P_{cv}^{\sigma}\right|^2 = \left|I_{cv}\right|^2 M^2 \quad (3)$$

where I_{cv} represents the overlap integral between the envelope functions of an electron and a hole, and

$$M^2 = \frac{m_0^2}{12 m_e^*} \cdot \frac{E_g (E_g + D)}{E_g + 2D/3} \quad (4)$$

as derived by the first-order k.p is the interaction between the conduction band and valence band. Here, E_g is the band gap, m_e^* is the electron effective mass, D is the spin-orbit interaction energy of the QD material. Equation 3 holds as long as we consider QDs with a nearly symmetrical shape [11]. In actual SAQD-LDs, we should rewrite the linear optical gain formula of equation (1) by taking into account inhomogeneous broadening due to the QD size and composition fluctuation in terms of a convolution integral as

$$g^{(1)}(E) = \frac{2\pi e^2 \hbar N_D}{c n_r e_0 m_0^2} \int_{-\infty}^{\infty} \frac{\left|p_{cv}^{\sigma}\right|^2}{E_{cv}} (f_c(E') - f_v(E')) \times B_{cv}(E - E') G(E' - E_{cv}) dE' \quad (5)$$

where E_{cv} is the center of the energy distribution function of each interband transition, $f_c(E')$ is the electron occupation function of the conduction-band discrete state of the QDs with the

interband transition energy of E', and $f_v(E')$ is that of the valence band discrete state. The energy fluctuation of QDs are represented by $G(E'-E_{cv})$ that takes a Gaussian distribution function as

$$G(E'-E_{cv}) = \frac{1}{\sqrt{2\pi}\xi_0}\exp(-(E'-E_{cv})^2/2\xi_0^2) \quad (6)$$

Whose FWHM is given by $G_0 = 2.35x_0$. The width G_0 usually depends on the band index c and v [6].

The most popular and useful way to deal with carrier and photon dynamics in lasers is to solve rate equations for carrier and photons [9],[10],[11],[12],[13]. In our model, we consider an electron and a hole as an exciton, thus, the relaxation means the process that both an electron and a hole relax into the ground state simultaneously to form an exciton. We assume that the charge neutrality always holds in each QD.

In order to describe the interaction between the QDs with different resonant energies through photons, we divide the QD ensemble into j=1, 2,... 2M+1 groups, depending on their resonant energies for the interband transition over the longitudinal cavity photon modes. $j = M$ corresponds to the group and the mode with the central transition energy E_{CV}. We take the energy width of each group equal to the mode separation of the longitudinal cavity photon modes which equals to

$$D_E = ch/2n_r L_{ca} \quad (7)$$

where L_{ca} is the cavity length. The energy of the j[th] QD group is represented by

$$E_j = E_{cv} - (M - j)D_E \quad (8)$$

where $j = 1,2,...,2M+1$. The QD density j[th] QD group is given as

$$N_D G_j = N_D G(E_j - E_{cv})D_E \quad (9)$$

Let N_j be the carrier number in j[th] QD group, According to Pauli's exclusion principle, the occupation probability in the ground state of the j[th] QD group is defined as

$$P_j = N_j/2N_D V_a G_j \quad (10)$$

where V_a is the active region volume. The rate equations are as follows [9],[10],[11],[13],[14].

$$\frac{dN_s}{dt} = \frac{I}{e} - \frac{N_s}{\tau_s} - \frac{N_s}{\tau_{sr}} + \frac{N_w}{\tau_{we}} \quad (11)$$

$$\frac{dN_w}{dt} = \frac{N_s}{\tau_s} + \sum_j \frac{N_j}{\tau_e D_g} - \frac{N_w}{\tau_{wr}} - \frac{N_w}{\tau_{we}} - \frac{N_w}{\overline{\tau}_d}$$

$$\frac{dNj}{dt} = \frac{N_w G_j}{\tau_{dj}} - \frac{N_j}{\tau_r} - \frac{N_j}{\tau_e D_g} - \frac{c\Gamma}{n_r}.g^{(1)}(E)S_m$$

$$\frac{dS_m}{dt} = \frac{\beta N_j}{\tau_r} + \frac{c\Gamma}{n_r}.g^{(1)}(E)S_m - S_m/\tau_p$$

where N_s, N_w, and N_j are the carrier numbers in separate confinement heterostructure (SCH) layer, wetting layer (WL) and j[th] QD group, respectively, S_m is the photon number of m[th] mode, where m=1,2…2M+1, I is the injected current, G_j is the fraction of the j[th] QD group type within an ensemble of different dot size population, e is the electron charge, D_g is the degeneracy of the QD ground state without spin, b is the spontaneous-emission coupling efficiency to the lasing mode. $g_{mj}^{(1)}$ is the linear optical gain which the j[th] QD group gives to the m[th] mode photons where is represented by

$$g_{mj}^{(1)}(E) = \frac{2\pi e^2 \hbar N_D}{c n_r \varepsilon_0 m_0^2} \cdot \frac{\left|p_{cv}^{\sigma}\right|^2}{E_{cv}} (2p_j - 1). \quad (12)$$
$$G_j B_{cv} (E_m - E_j)$$

the related time constants are as τ_s, diffusion in the SCH region, τ_{sr}, carrier recombination in the SCH region, τ_{we}, carrier reexcitation from the WL to the SCH region, τ_{wr}, carrier recombination in the WL, τ_{dj}, carrier relaxation into the j[th] QD group, τ_r, carrier recombination in the QDs, τ_p, photon lifetime in the cavity, The average carrier relaxation lifetime, $\bar{\tau}_d$, is given as

$$\tau_d^{-1} = \sum_j \tau_{dj}^{-1} G_j = \tau_{d0}^{-1}(1 - P_j)G_j \quad (13)$$

where τ_{do} is the initial carrier relaxation lifetime. The photon lifetime in the cavity is

$$\tau_p^{-1} = (c / n_r)[\alpha_i + \ln(1/R_1 R_2)/2L_{ca}] \quad (14)$$

where R_1 and R_2 are the cavity mirror reflectivities, and a_i is the internal loss. The laser output power of the m[th] mode from one cavity mirror is given a

$$I_m = \hbar \omega_m c S_m \ln(1/R)/(2L_{ca} n_r) \quad (15)$$

where w_m is the emitted photon frequency, and R is R_1 or R_2. We solved the rate equations numerically using fourth order Runge-Kutta method to characterize static characteristics of InAs/AlGaAs broadband self-assembled QD lasers by supplying the step-like current at the time of $t = 0$. The system reaches the steady-state after finishing the relaxation oscillation.

3. Simulation Results

Figure 1 shows light-current (L-I) characteristics of the mentioned self-assembled QD laser diode (SAQD-LD) for FWHM of IHB (a) $G_0 = 60meV$ at $\hbar\gamma_{cv} = 15, 20, 30,$ and $60meV$, and (b) $G_0 = 80meV$ at $\hbar\gamma_{cv} = 20, 30, 40,$ and $50meV$,

As we can see from Figure 1, non-linear L-I characteristics exist when HB is smaller than IHB. While when the HB becomes equal to IHB, L-I curve has a linear shape. For large HBs, near to IHB up to a bit larger than IHB, output power increases infinitely as the injected current elevates. Besides, Slope efficiency (external quantum differential efficiency) heightens as the HB increases up to the IHB. In addition, when the HB exceeds the IHB, static-characteristics degrade. We can conclude that the broadband SAQD-LD has its best performance when HB is equal to IHB.

Furthermore, Figure 1 shows that slope efficiency decreases and threshold current also elevates with enhancement of IHB as a result of decreasing the central group density of states (DOS). In some cases such as Figure 1(a) for FWHM of HB 30 meV and at I = 2.5 mA or Figure

1(b) for FWHM of HB 40 meV and at I = 3.5 mA, all of the central group DOS occupies and the output power reaches its maximum amount, then, it decreases as the injected current increases, as a result of emitting of central group carriers within other modes.

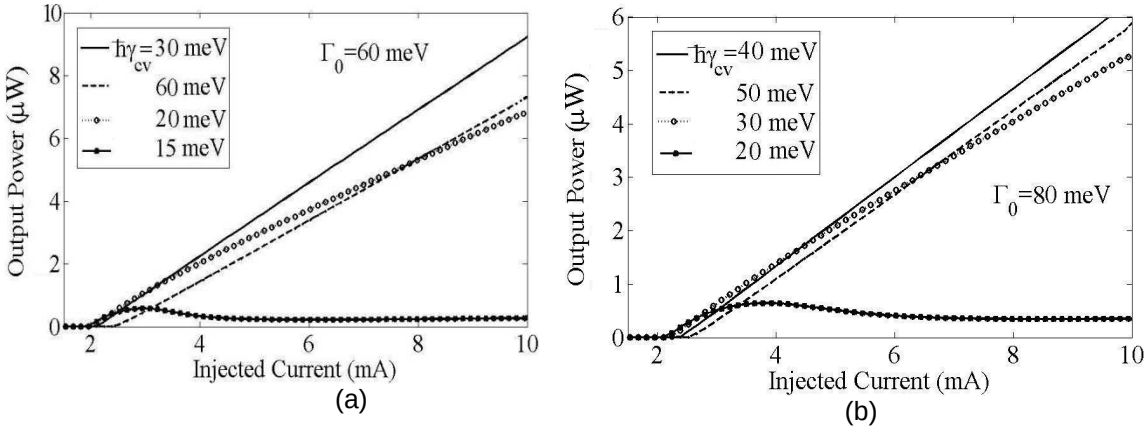

Figure 1. Light-current characteristics of InAs/AlGaAs broadband SAQD-LD for FWHM of IHB and HB (a) $G_0 = 60meV$ and $2\hbar\gamma_{cv} = 30, 40, 60, and\ 120\,meV$ and (b) $G_0 = 80meV$ at $2\hbar\gamma_{cv} = 40, 60, 80, and\ 100\,meV$.

In addition, the threshold current increase as the HB increases owing to elevating DOS of the central group. This fact is revealed clearly in Figure 2 where L-I characteristics is shown for HB 0.8 and 80 meV. It is clearly shown that slope efficiency and the threshold current enhance with increase of HB. Figure 3 shows L-I characteristics for QD coverage as a variable parameter $\xi = 0.04, 0.07, 0.1, 0.2, 0.4, and\ 0.8$ and carrier radiative recombination times 2.8 ns in QDs and 3ns in WL.

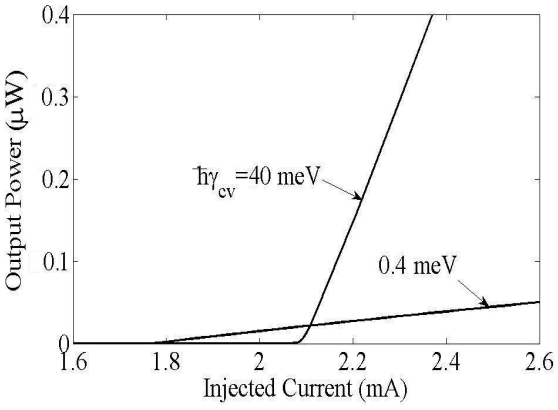

Figure 2. Output power as a function of injected current for HB 0.8 and 80 meV

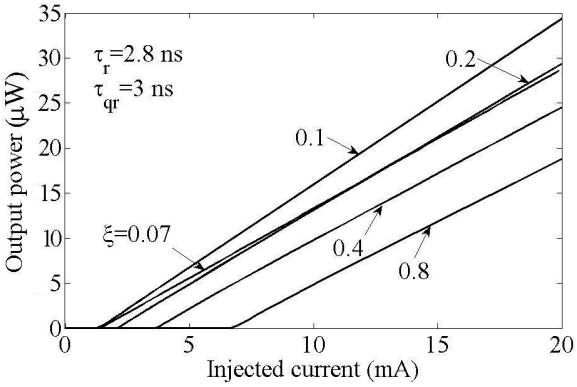

Figure 3. shows L-I characteristics for QD coverage as a variable parameter $\xi = 0.04, 0.07, 0.1, 0.2, 0.4, and\ 0.8$

As shown in Figure 3, with increase of QD coverage from 0.1, threshold current increases owing to enhancing the number of QDs or the QD volume (the number of energy levels) and as a result, it is required to provide more QD carriers in order to establish population inversion. Besides, output power and slope efficiency decline due to decreasing occupation probability and accordingly, increasing the relaxation time. It is clearly revealed that the QD coverage 0.1 has the best L-I characteristics and the lowest threshold current. It is concluded that there is an optimum QD coverage.

4. Conclusion

Considering energy level and size distributions of InAs/AlGaAs broadband self-assembled quantum-dots, we solved the rate equations numerically using fourth-order Runge-Kutta method and simulated light-current characteristics of the mentioned SAQD-LD. Simulated results of the static-characteristics showed that slope efficiency elevates as the HB increases whereas it becomes equal to IHB. Exceeding the HB from IHB and elevating IHB result in degradation of light-current characteristics. Threshold current increases as the HB and IHB enhance. Nonlinearity appears in light-current characteristics whereas HB becomes equal to IHB. The SAQD-LD has the best performance when HB

is equal to IHB. We also saw that increasing of HB from IHB leads to declining of static-characteristics of InAs/AlGaAs broadband SAQD-LD. We revealed that there is an optimum QD coverage in which the SAQD-LD operates with lowest possible threshold current and maximum output power as whatever the QD coverage enhances from that optimum amount, the threshold current increases and slope efficiency decreases.

References

[1] Liu N, Jin P, Wang Z. InAs/GaAs quantum-dot super luminescent diodes with 110 nm bandwidth. Electron. *Lett*. 2005; 41: 1400- 1402.

[2] Lv X, Liu Q, Jin P, Wang Z. Broadband emitting super luminescent diodes with InAs quantum dots in AlGaAs matrix. *IEEE Photon. Technol. Lett*. 2008; 20: 1742-1744.

[3] Zhang Z, Wang Y, Xu B, Liu F. High performance Quantum-dot superluminescent diodes. *IEEE Photon. Technol. Lett.* 2004; 16: 27-29.

[4] Zhang Y, Hogg P Jin, Wang Z. High power quantum-dot superluminescent LED with broadband drive current insensitive emission spectra using tapered active region. *IEEE Photon. Technol. Lett.* 2008; 20: 782-784.

[5] Sugawara M, Mukai K, Shoji H. Effect of phonon bottleneck on quantum-dot laser performance. *Applied Phys. Lett*. 1997; 71: 2791-2793.

[6] Sugawara M. Self -Assembled InGaAs/GaAs Quantum Dots. Academic Press 60. 1999.

[7] Sun Z, Ding D, Gong Q, W Zhou, B Xu, Wang Z. Quantum-dot superluminescent diode: A proposal for an ultra-wide output spectrum. *Opt. Quantum Electron*. 1999; 31: 1235-1246.

[8] Djie HS, Ooi B, Fang, Wu XY, Fastenau J, Liu X, Hopkinson M. Room-temperature broadband emission of an InGaAs/GaAs quantum dots laser. *Opt. Lett.* 2007; 32: 44-46.

[9] Tan C, Wang Y, Djie H, Ooi B. Role of optical gain broadening in the broadband semiconductor quantum-dot laser. *Applied Phys. Lett*. 2007; 91: 061117-061119.

[10] Tan C, Wang Y, Djie H, Ooi B. The role of optical gain broadening in the ultrabroadband InGaAs/GaAs interband quantum-dot laser. *Comput. Matter. Sci.* 2008; 44: 167- 173.

[11] Sugawara M, Mukai K, Nakata Y, Ishikawa H. Effect of homogeneous broadening of optical gain on lasing spectra in self-assembled InxGa1ÀxAsÕGaAs quantum dot lasers**.** *Phys.Rev. B.* 2000; 61**:** 7595-7603.

[12] Grundmann M.. Nano Optoelectronics. New York: Springer. 2002.

[13] Markus A, Chen J, Gauthier-Lafaye O, Provost J, Paranthoen C, Fiore A. Impact of Intraband relaxation on the performance of a quantum-dot laser. *IEEE J. Sel. Top., Quantum electron.* 2003; 9: 1308-1314.

[14] Sugawara M, Hatori N, Ebe H, Ishida H. Modeling room-temperature lasing spectra of 1.3µm self-assembled InAs/GaAs quantum-dot lasers: Homogeneous broadening of optical gain under current injection. *Applied Phys*. 2005; 97: 043523-043530.